

A major purpose of the Technical Information Center is to provide the broadest dissemination possible of information contained in DOE's Research and Development Reports to business, industry, the academic community, and federal, state and local governments.

Although a small portion of this report is not reproducible, it is being made available to expedite the availability of information on the research discussed herein.

1

Los Alamos National Laboratory is operated by the University of California for the United States Department of Energy under contract W-7405-ENG-36

LA-UR--89-2734

DE89 016595

TITLE PRELIMINARY REPORT ON CONFINED TENSION TESTING OF 900-24

AUTHOR(S) Richard A. Harlow
Richard V. Browning
Analysis and Testing, WX-11

SUBMITTED TO Western Regional Strain Gauge Committee Meeting
Idaho Falls, ID
22 August 1989

In preparation of this article the publisher recognizes that the U.S. Government retains a nonexclusive, royalty-free license to publish or reproduce the published form of this contribution or to allow others to do so, for U.S. Government purposes.

The Los Alamos National Laboratory requests that the publisher identify this article as work performed under the auspices of the U.S. Department of Energy.

Los Alamos National Laboratory
Los Alamos, New Mexico 87545

MASTER

**Preliminary Report on Confined Tension
Testing of 900-24**

Richard A. Harlow
Richard V. Browning
Analysis and Testing WX 11

September 19, 1988

CONTENTS

I.	INTRODUCTION	1
II.	DESIGN OF CONFINING PRESSURE VESSEL	2
III.	CALIBRATION AND VERIFICATION TESTS	3
IV.	EXPLORATORY TESTS ON 900-24	7
V.	COMMENTS ON RESULTS	9
VI.	REFERENCES	11
	Appendix A. DETAILS OF DATA REDUCTION METHODS	13
	Appendix B. ORIGINAL TEST RESULTS	15

LIST OF FIGURES

1	Nominal specimen geometry	2
2	Pressure Vessel	4
3	Internal Load cell	6
4	Test 900CT5	8
5	Test 900CT1	16
6	Test 900CT2	16
7	Test 900CT3	17
8	Test 900CT4	17
9	Test 900CT5	18
10	Test 900CT6	18
11	Test 900CT7	19
12	Test 900CT8	19
13	Test 900CT9	20
14	Test 900CT10	20
15	Test 900CT11	21
16	Test 900CT12	21
17	Test 900CT13	22

LIST OF TABLE

1	Failure table	9
2	Failure table ordered by stress	10

Preliminary Report on Confined Tension Testing of 900-24

by

Richard A. Harlow
Richard V. Browning
Analysis and Testing WX-11

ABSTRACT

A specially designed confining pressure vessel is described that allows tensile samples to be tested under a superimposed confining hydrostatic pressure. Tests on samples of well characterized materials such as aluminum were used to verify the operation of the system, calibration of the internal load cell, and data reduction methods. The results of a series of exploratory tests done on the inert material 900-24 are described.

I. INTRODUCTION

Evidence of cracking in high-explosive (HE) charges during early tests on EPW systems coupled with failures observed in previous programs prompted Paul Smith, WX 11, to instigate a small research program to study the failure behavior of HE materials and their inert simulator under a superimposed hydrostatic state of loading. Bridgman^{1,2} and other people³ performed compression tests under hydrostatic loading on many brittle materials and found a significant change in their apparent ductility. Bridgman's work was well known to many people but the application of his results was limited to intuitive explanations of differences between numerical results and observations from system tests.

Unfortunately the complexity of doing fracture or failure oriented tests has inhibited work on HE materials except for the standard tension test which is very poor for evaluating fracture sensitivity. A complete study of the fracture behavior of HE, not including hydrostatic pressure effects, could be very expensive and time consuming as well. The compact fracture toughness specimen usually used



Figure 1: The specimen geometry used is similar to an ASTM E-8 sample.

for evaluating metallic materials is a complex design, difficult to machine and requires cyclic loading to develop a natural fatigue crack before performing the actual test. Furthermore, we do not have appropriate machines for this type of testing on HE.

At Smith's suggestion we finally decided to begin with Bridgman style hydrostatically confined compression tests, including the capability of doing tension tests as well through the use of a necked down specimen. One author (RAH) designed the confining pressure vessel, developed the associated control and data acquisition techniques and performed the actual tests. The other author (RVB) checked the data reduction methods and devised some of the interpretations of the the results.

II. DESIGN OF CONFINING PRESSURE VESSEL

In designing the confining pressure vessel several factors were considered. A standard sized cylindrical necked tension specimen geometry was selected, see Fig. 1. This, along with the need to accommodate strain measuring instrumentation on the sample, dictated the internal dimensions of the vessel, see Fig. 2. Another major factor was the maximum internal or confining pressure at which to test. We decided that a maximum confining pressure of 10,000 psi was required. The vessel also had to have a means for applying an external axial force to the sample through a sealed plunger as well as incorporating a multi-conductor electrical feedthrough for internal instrumentation. The testing was to be performed as an attended operation, that is with personnel present, so the vessel had to be designed with a reasonable safety factor.

In the vessel design the maximum stresses occur in the tangential or hoop direction. At the 10,000 psi maximum working pressure the calculated hoop stress

was about 28,000 psi. At a 25,000 psi internal proof test pressure the stress becomes about 69,500 psi. The material chosen for the confining pressure vessel was A340 steel with a yield strength of about 70,000 psi in an annealed condition. With this material at the 10,000 psi pressure the hoop stress is about 40% of the yield strength. At the 25,000 psi proof pressure the hoop stress is nearly equal to the yield strength. No heat treatment was specified for the vessel.

Before using the pressure vessel for attended testing a proof test was performed. The vessel was instrumented with strain gages on the outside surface in two locations. One biaxial gage was placed on the center of the length of the vessel body measuring strain in both hoop and axial directions. The other gage, again a biaxial gage measuring both hoop and axial strain, was placed on the outside surface over the end seal area where the vessel wall thickness is at a minimum. The vessel was then placed in a coffin, for containment in the event of a failure, and internal pressure applied. The hydraulic media for the proof test was Dow Corning DC200 fluid, a 20 centistoke silicone oil. The internal pressure was raised to 25,000 psi while monitoring the strain gage response. The pressure was held at about 25,000 psi for a period of about 5 minutes. The gages showed a small amount of plasticity on the external surface indicating even greater yielding on the internal surface where the stresses are theoretically higher. The plastic strain was small, however, and the vessel did not fail or leak, indicating that 10,000 psi (40% of the proof pressure) was a safe maximum working pressure.

III. CALIBRATION AND VERIFICATION TESTS

In conducting the confined tensile testing three measurements were required, the internal confining pressure, the axial strain on the surface of the sample and the reacting force applied to the sample to maintain hydrostatic stress. The measurement of the confining pressure was done with a strain gaged diaphragm pressure transducer commercially available in conjunction with the recommended signal conditioning. This was by far the easiest of the three measurements to make. The measurement of the axial strain was performed with a strain gage extensometer, again commercially available. The calibration and verification of the extensometer was more complex than that of the pressure transducer. In addition to a simple calibration of output voltage versus displacement at 0 psig., verification tests were conducted to determine the extensometer response to pressure.

In order to determine this response two tests were conducted. In the first test the extensometer was pinned, or mechanically restrained, to allow no displacement and then hydrostatic pressure applied. A linear fit of the extensometer response to

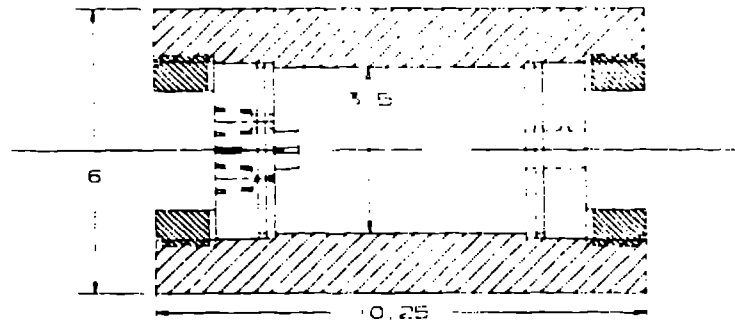


Figure 2: The basic pressure vessel consists of the cylinder, two end plugs and their retaining rings. O-Rings are used in the plugs to provide the pressure seal. Electrical feedthroughs for the extensometer wiring are in one plug, while the other has a through hole to receive the plunger.

pressure was made for possible use as a correction factor in subsequent tests. In the next test the extensometer was attached to an aluminum sample with a smaller diameter gage section than the 900-24 samples. A smaller diameter was used to compensate for the difference in strength and stiffness between the aluminum and the 900-24. The instrumented aluminum sample was placed in the vessel and hydrostatic pressure applied. A reacting force was applied to the end of the sample during pressurization in order to maintain a hydrostatic stress state. The force was applied through a plunger in the end of the vessel by an Instron Corp. electro-mechanical load frame and measured externally using the Instron load cell. The reacting force was applied as a function of the confining pressure by a computer controlled closed loop system. Upon reaching 10,000 psi the reacting axial force was reduced to develop an axial tensile strain. Standard three dimensional linear elastic stress-strain equations were used to compute theoretical strain from the recorded load and pressure values. An attempt was made to correct for changes in extensometer output due to pressure that were discovered in the first test. It was apparent from this correction that the correspondence to theoretical values was substantially worsened. We believe that in the first test the extensometer was not actually confined to zero displacement by the retaining pin, as originally assumed, and the change in extensometer output was due to displacement within the confining mechanism. The correspondence to theoretical values of the data from the test with the extensometer attached to the aluminum sample without

the correction was very good and it was felt that at pressures up to 10,000 psi the extensometer would be accurate enough to use for subsequent tests.

After confirming that strain measurements using the extensometer could be made in the high pressure environment of the vessel, preliminary tests with 900-24 began. Fig. 1 shows the nominal dimensions of the specimens. It was originally thought that the friction of the plunger, applying the reacting force, moving through the plunger seal would be insignificant. After conducting several confined tensile tests with the 900-24 material, and obtaining unexpected results, it was evident that the seal friction was much greater than expected. Tests were conducted to determine seal friction as a function of internal pressure. The results of these tests indicated that at 10,000 psi the frictional force required to move the plunger through the seal was about twice that required to break the samples of 900-24 in tension with no confining pressure. As the force measurement used to calculate the axial stress in the sample was external to the vessel, the measurement included the seal friction component. The repeatability of the seal friction was not consistent enough to allow for mathematical correction. An alternative to mathematical correction of the seal friction induced error was to make the reacting force measurement on the other side of the seal, that is inside the pressure vessel. In this way the reacting force applied to the sample could be measured without the seal friction component.

A new plunger was designed that incorporates a relatively small cross sectional area with an enlarged diameter vent passage, see Fig. 3. The intent was to maximize, within safe limits, axial stress in the plunger for greater strain sensitivity and still be able to reasonably install strain gages on the inside surface of the vent passage. Placing the strain gages on the inside surface of the vent passage isolates the gages from the high pressure environment as well as simplifying assembly and disassembly of the vessel for installing new test samples.

After instrumenting the redesigned plunger a program of calibration and verification was initiated. The first step in this program was to perform a simple output voltage versus axial force calibration to determine the sensitivity of the instrumented plunger to force and determine linearity and repeatability. Axial force was applied to the plunger using the Instron load frame and measured with the Instron load cell. The plunger output response as well as the Instron load cell were recorded for determination of the plunger sensitivity, linearity and repeatability. After confirming the linearity and repeatability of the plunger and calculating the sensitivity to axial force verification at high pressure began. The method used to verify the usefulness of the plunger for high pressure testing was much the same

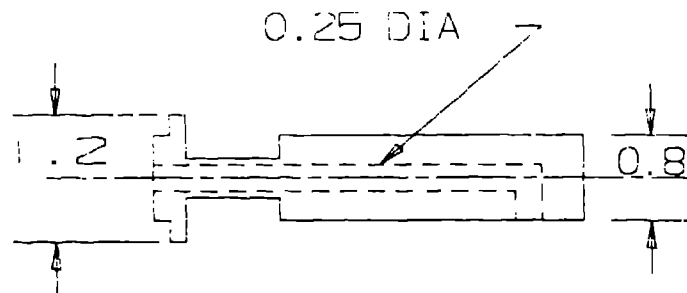


Figure 3: Design of the instrumented axial load plunger. Strain gages internally mounted in the reduced section of the plunger avoid the seal friction forces and measure actual specimen axial loads.

as used to qualify the extensometer. An aluminum sample was used, this time of the same geometry as the 900-24 samples. The sample was instrumented with the extensometer, placed in the vessel and the vessel assembled with the instrumented plunger. The pressure was increased to 10,000 psi while applying the reacting load with the Instron as a function of pressure to maintain a hydrostatic stress state. The internal pressure, the extensometer response, the plunger output and the external force were all recorded in this test. Results showed that the plunger output response was much lower than expected based on the other measurements and the same three dimensional linear elastic stress-strain equations. After further analysis of the system it was determined that correction for hydrostatic pressure acting on the instrumented plunger must be made. The pressure acting on the plunger caused hoop stress in the instrumented section of the plunger and through the Poisson effect caused a tensile strain in the section. This tensile strain was subtracting from the compressive strain induced by the axial compressive force. Another component affecting the plunger was the internal pressure acting on the area differential of the plunger. This also caused tensile strain in the plunger subtracting from the desired compressive strain used to measure the reacting axial force inside the vessel. After mathematically correcting for both of these conditions the correspondence of the plunger response to theoretical values of the aluminum response was very good. The difference between measured internal and external forces also agreed very well with seal friction values measured earlier. In the origi-

nal verification of the extensometer using the aluminum sample the forces required to induce an equivalent strain were much higher than required for the 900-24 material. Because of this the seal friction component was a much smaller percentage of the total force and could be neglected. The final verification test indicated that both the extensometer and the instrumented plunger would be accurate enough to continue testing with the 900-24 material.

IV. EXPLORATORY TESTS ON 900-24

As of this writing a total of thirteen tests have been conducted on 900-24 inert material. Two of these tests were invalidated because of hardware problems, such as leaks, or operator error. All tests have been conducted using DC200 fluid, the same media as used in the proof test of the vessel. The first four tests conducted (one of these was invalid) were done using the 900-24 material in an untreated condition as they were received. These tests indicated that the material was failing when the axial stress and the axial strain were still very much compressive. Upon examination of the broken samples the failure surfaces appeared the same as if the samples had failed in tension.

This behavior was not expected and so the next tests were conducted on 900-24 samples that had been coated with various materials. The reason for coating the samples was that we believed the silicone oil was intruding into the material. The inert material is basically a mixture of relatively high modulus crystals bonded together with a relatively low modulus plastic binder. The hypothesis was that the silicone oil under pressure was displacing the softer binder and changing, locally, the surface of the material by opening a small crack. Once the crack, or opening between crystals, was initiated it would expose progressively more surface area to the pressurized silicone oil, causing a very localized stress concentration which, once started, would become a self supporting fracture. This type of failure would appear to be, and actually would be, a tensile failure.

Upon testing the samples that had been coated with various materials it was observed that a significant change in strain at failure occurred. Table 1 presents a summary of these initial test results. For example, compare the results for tests 900ct1 and 900ct3, both for uncoated material, with results from 900ct10, a Krylon coated specimen tested at the same nominal pressure. The greater difference between pressure and failure stress indicates much improved performance. The complete stress-strain curves are displayed in Appendix B. A typical result curve, with the extraneous data points following fracture removed, is shown in Fig. 4.

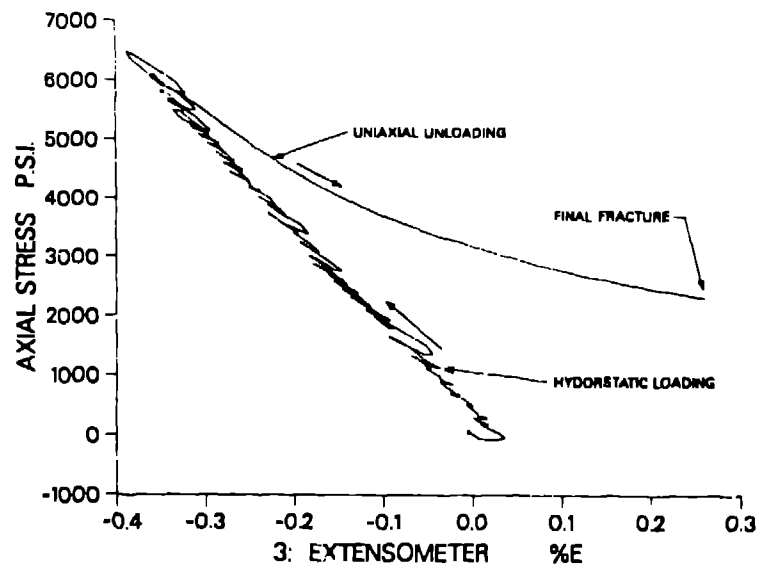


Figure 4: Test of Krylon coated sample with extraneous data points following fracture removed. The initial hydrostatic loading curve is rough because of the confining pressure is ramped up using a hand pump. Positive stress is compressive in this graph.

Table 1: Test summary. The total strain at failure is given by ϵ_f and the corresponding stress is σ_f . Note that the relative strength of the sample is given by the difference (actually the sum using the sign convention of the table) between the pressure and the failure stress in this loading situation. Positive pressure is compressive. Positive failure stress, σ_f , is tensile.

Test	Coating	Pressure (psi)	ϵ_f (%)	σ_f (psi)
900ct1	none	10000	-0.170	-6800
900ct2	bad test			
900ct3	none	10000	-0.225	-7700
900ct4	none	5200	-0.045	-2900
900ct5	Krylon	6500	+0.290	-2250
900ct6	M-Coat D	6500	+0.120	-2200
900ct7	M-Coat A	6500	+0.030	-3500
900ct8	Tens-Lac under.	7000	-0.010	-3000
900ct9	Vinyl tape	8000	-0.170	-5000
900ct10	Krylon	10000	-0.130	-5200
900ct11	bad test			
900ct12	Tens-Lac u+ov.	7250	-0.040	-2900
900ct13	none	725	+0.075	+150

The sensitivity to confining pressure level seems to support the original hypothesis of oil intrusion onto the material.

More test samples of 900-24 material are currently being produced and a program of testing both uncoated and coated samples at different levels of confining pressure will be initiated to better characterize the material behavior in a hydrostatically stressed environment.

V. COMMENTS ON RESULTS

Test results to date indicate that samples coated with a rigid material, like the acrylic Krylon, are apparently much more resistant to fracture than uncoated specimens. Rough estimates can be made by calculating equivalent uniaxial stresses and strains from the test data. Table 2 shows these calculated numbers ordered by equivalent stress together with a very rough estimate of the shear modulus of the coating. We have no direct method of measuring modulus of a thin film. We are basically trying to distinguish between soft rubbery materials like RTV silicones and stiff materials like polycarbonate and PMMA. Also note the considerable sample to-sample variation and confining pressure effects observable in the

Table 2: Test results ordered by equivalent stress at failure calculated as $\sigma_{eq} = p + \sigma_f$. The relative stiffness is our estimate of the shear modulus of the coating, high = 10^5 - 10^6 psi, low = 0 - 10^4 psi. The equivalent uniaxial strain, $\Delta\epsilon$ is calculated as the difference between the extensometer reading at failure and the reading before starting the uniaxial unloading.

Test	Coating	σ_{eq} (psi)	$\Delta\epsilon$ (%)	Rel. Stiffness
900ct10	Krylon	4800	0.404	high
900ct12	Tens-Lac u+ov.	4350	0.344	high
900ct6	M-Coat D	4300	0.576	high
900ct5	Krylon	4250	0.671	high
900ct8	Tens-Lac under.	4000	0.364	?
900ct1	none	3200	0.211	low
900ct7	M-Coat A	3000	0.252	low
900ct9	Vinyl tape	3000	0.314	low
900ct3	none	2300	0.164	low
900ct4	none	2300	0.151	low
900ct13	none	875	0.133	low

results for uncoated specimens and the two Krylon coated specimens.

In an HE system, potted in a typical silicone rubber, and then subjected to high acceleration levels the stress state around the HE surface of the charges will be close to that encountered in our hydrostatic tests in the sense that the shear stresses are low compared with the pressures involved. Typical silicone rubber potting materials have a very low shear modulus compared to the HE and could intrude into the HE surface in precisely the same fashion as the silicone oil in our experiments.

We recommend coating charges with a selected material in a future Davis gun test to evaluate this theory. A brittle stress coating was applied in one early Davis gun tests and in that test no cracking of the inert was observed. In our tests the brittle stress coatings were not quite as effective as Krylon but did enhance the apparent ductility of the the samples.

Additional tests on other coatings are planned for the near future. We do believe that improvements in the apparent strain to failure, or ductility, of HE like materials could be realized. Dramatic improvements in the stress at failure is not likely because this is basically controlled by the shear strength of the HE and not substantially changed by the coatings.

VI. REFERENCES

1. P. W. Bridgman, *Studies in Large Plastic Flow and Fracture*, McGraw-Hill, New York, 1952.
2. P. W. Bridgman, "Fracture and Hydrostatic Pressure," in *Fracturing of Metals*, American Society for Metals, Cleveland, 1947, pp. 246-261.
3. William F. Brace, "Brittle Fracture of Rocks," in *State of Stress in the Earth's Crust*, W. R. Judd (Ed.), Elsevier, New York, 1964, pp. 111-178.
4. R. J. Roark and W. C. Young, *Formulas for Stress and Strain*, 5th ed., McGraw-Hill, New York, 1975.

Appendix A. DETAILS OF DATA REDUCTION METHODS

When a uniform pressure is applied to the side, but not the ends, of a necked tensile specimen the axial stress in the reduced diameter section of the sample is

$$\sigma_p = (A_{2s} - A_{1s})P/A_{1s}.$$

where

$$\begin{aligned}\sigma_p &= \text{Pressure Induced Axial Stress,} \\ A_{1s} &= \text{Sample Small Diameter Area,} \\ A_{2s} &= \text{Sample Large Diameter Area,} \\ P &= \text{Applied Pressure.}\end{aligned}$$

When a reacting force is applied to the free end of the sample a hydrostatic stress state may be maintained. The total stress is

$$\sigma = (A_{2s} - A_{1s})P/A_{1s} - F/A_{1s}.$$

where

$$F = \text{Applied Force.}$$

After achieving a confining pressure of interest the reacting force may be reduced to create axial tensile stress in the sample at any level of confining pressure.

The axial force is determined by measuring the strain in the plunger and applying corrections to compensate for pressure effects. The total axial strain is the sum of three terms; one from the axial load on the end of the plunger, a second caused by the Poisson effect from the hoop stress generated by the confining pressure, and a third term coming from the pressure acting axially on the area differential between the end of the plunger (major diameter) and the outer diameter of the reduced section. The second term is obtained from standard thick walled cylinder equations, see p. 504 in Roark⁴. Writing out this equation we have

$$\epsilon_{total} = \frac{F}{\pi L R_1^2} \frac{1}{E} \frac{1}{R_1^2} + \frac{\nu P}{L} \frac{2R_2^2}{R_2^2 - R_1^2} \frac{1}{E} + \frac{P}{L} \frac{R_2^2 - R_1^2}{R_2^2 - R_1^2}$$

Then solving for F and defining $K = \pi L (R_2^2 - R_1^2)$ we have

$$F = K \epsilon_{meas} = \frac{K P}{E} \left(\frac{2\nu R^2}{R_o^2 - R_i^2} + \frac{R_o^2 + R_i^2}{R_o^2 - R_i^2} \right)$$

where

K = Strain Sensitivity to Axial Force of Instrumented Plunger

ϵ_{meas} = Measured Axial Strain

E = Young's Modulus of Plunger

ν = Poisson's Ratio of Plunger

R_o = Outer Radius of Instrumented Section of Plunger

R_i = Inner Radius of Instrumented Section of Plunger

R_{maj} = Major Radius of Plunger

Appendix B. ORIGINAL TEST RESULTS

The figures shown here are unedited copies of stress strain curves from the original test series, including some tests where obvious errors occurred. Some figures are more difficult to interpret than others. Usually the post failure portion of the curve is clear, but sometimes it becomes confused with the original loading curve. In all cases the initial point is at the origin, and from there we trace the hydrostatic loading curve (usually very rough because of pressure loading with a hand pump) followed by a relatively smooth uniaxial stress unloading controlled by the Instron crosshead motion. Failure of the specimen is usually indicated by a sharp change in slope on the unloading curve, followed with several random data points.

Although not shown here, the confining fluid pressure does drop somewhat during the uniaxial unloading. In most cases the drop is less than 20%.

The complete time histories of load, pressure, sample strain, and other derived variables are available in QKPLT form for people interested in detailed study of these results.

900 24 Test 1 31 Mar 98

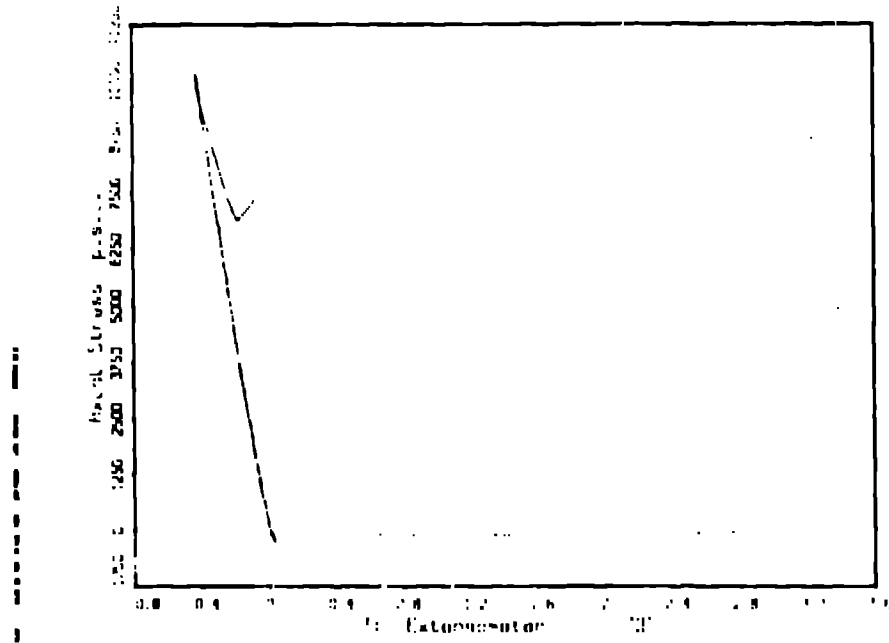


Figure 5: First Test of an uncoated specimen. Nominal pressure for uniaxial unloading, 10000 psi.

900 24 Test 2 31 Mar 98

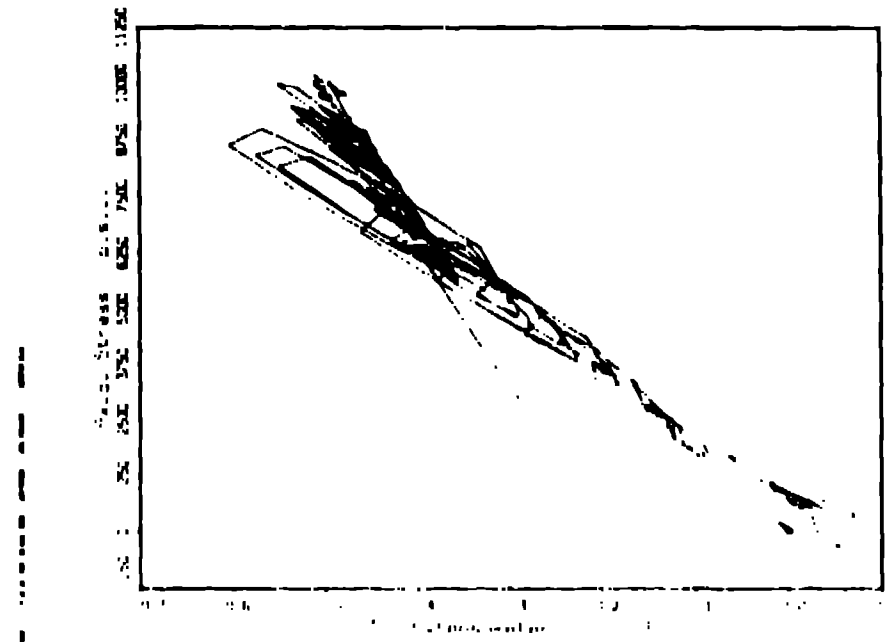


Figure 6: Example of a bad test. Usually we discard tests like this one

ACC 24 Test 4 - 1 Dec 68

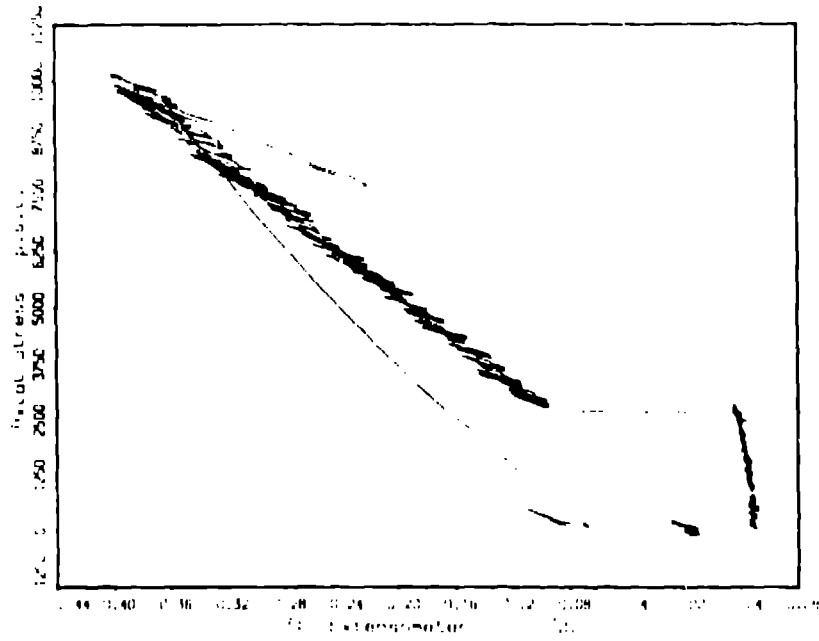


Figure 7: Uncoated specimen 2, 10000 psi.

ACC 24 Test 4 - 1 Dec 68

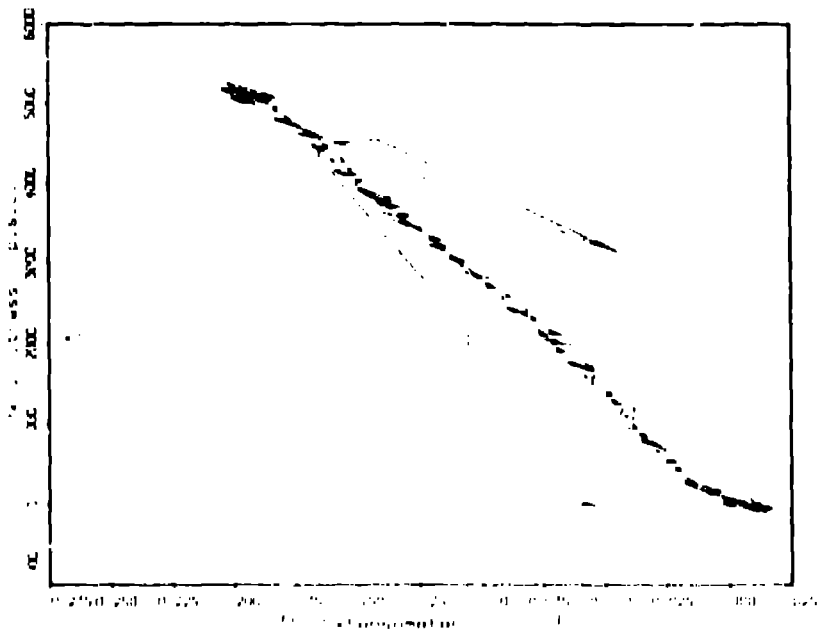


Figure 8: Uncoated specimen 3, 5200 psi.

800-24 Test 6 13 Apr 68

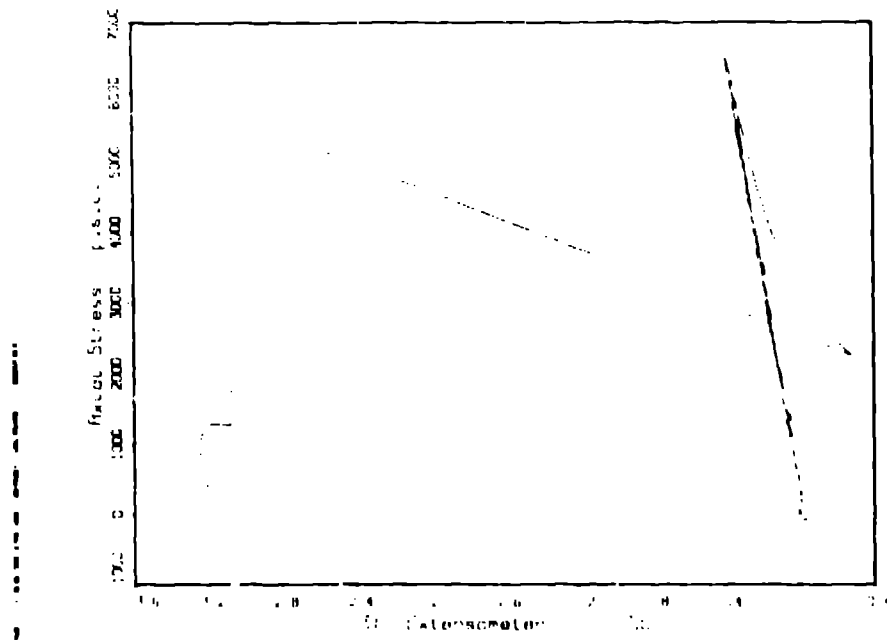


Figure 9: Kylon coated specimen, 6500 psi.

800-24 Test 6 13 Apr 68

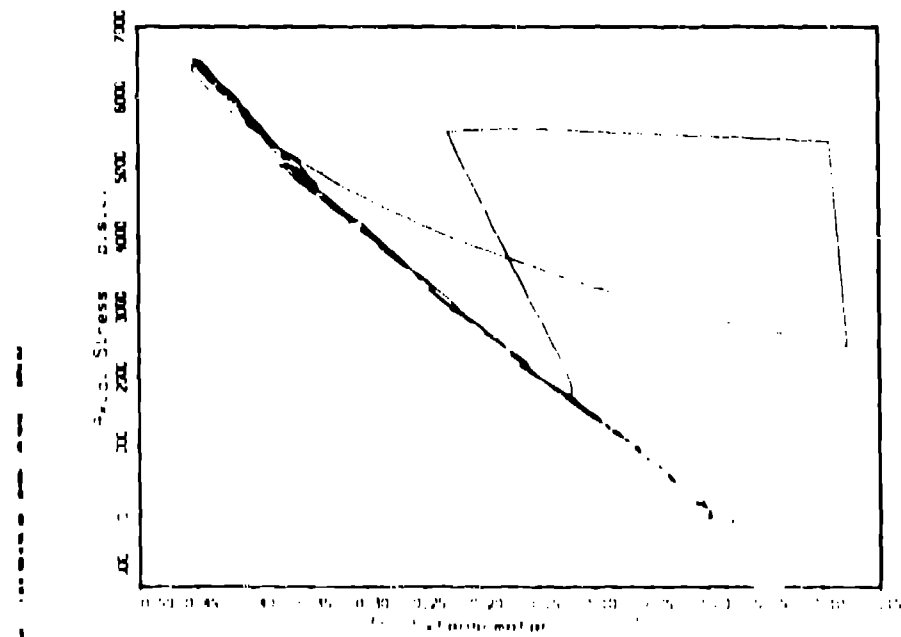


Figure 10: M Coat D, a strain gage coating material, 6500 psi.

900-24 Test 8 6 Apr 88

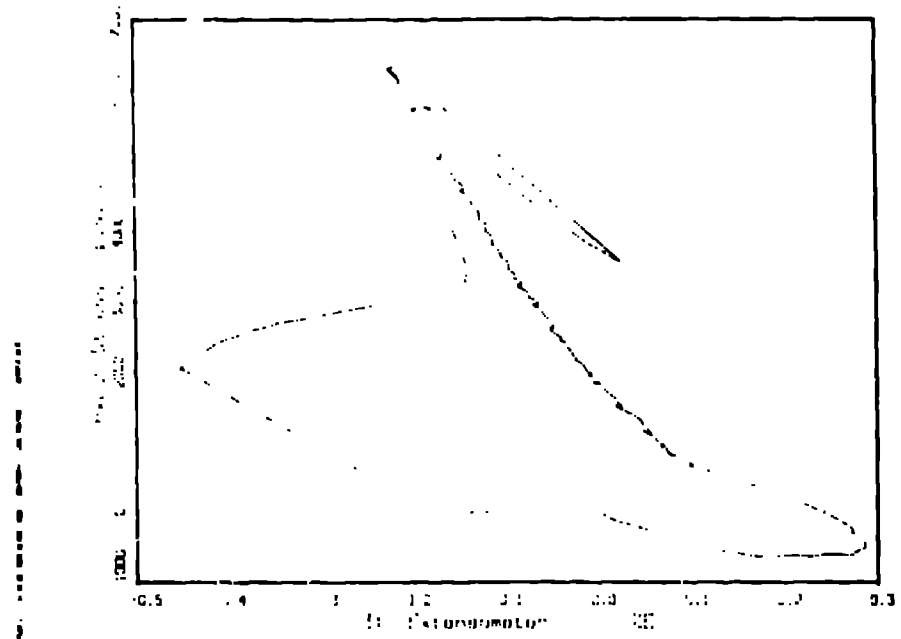


Figure 11: M-Coat A, another gage coating material, 6500 psi.

900-24 Test 8 6 Apr 88

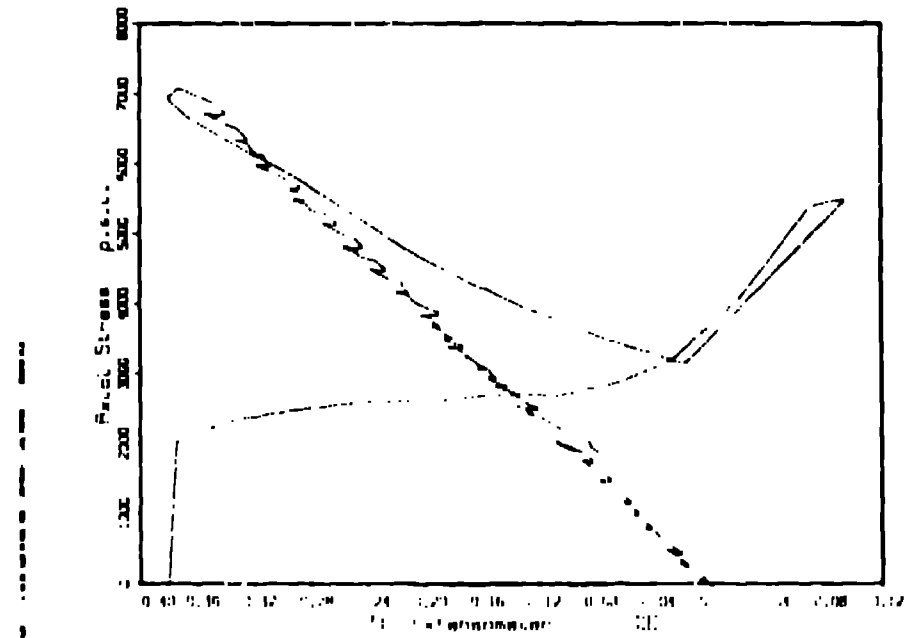


Figure 12: Tens-Lac undercoating, a brittle lacquer coating material used for whole field stress measurement, 7000 psi.

900-24 Test 10 7 Apr 88

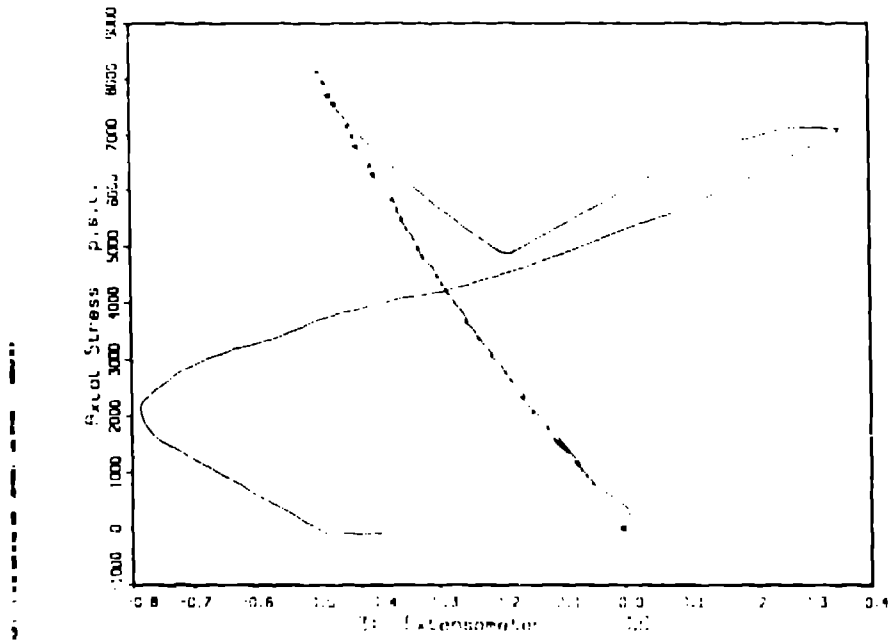


Figure 13: Vinyl tape, yellow, 8000 psi.

900-24 Test 10 7 Apr 88

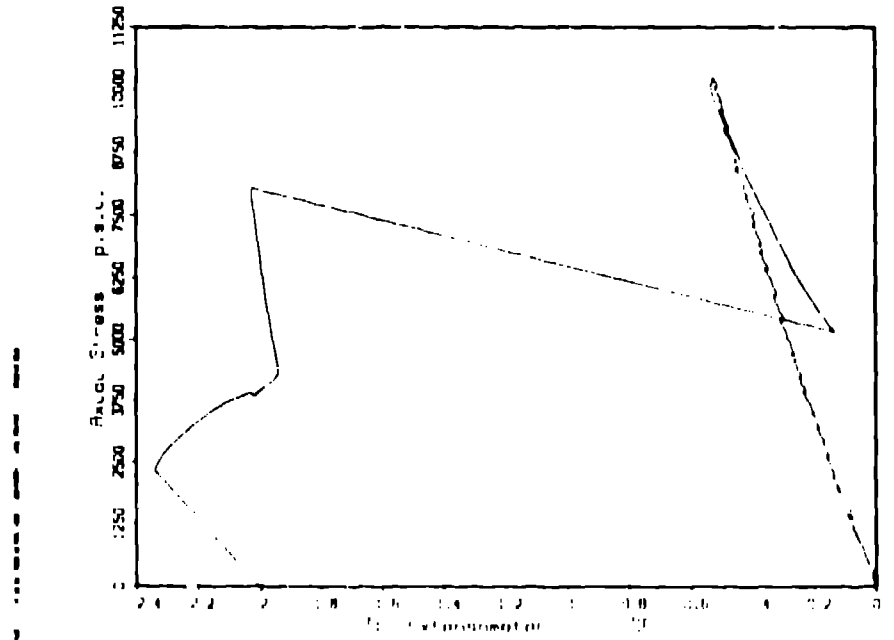


Figure 14: Krylon coated specimen 2, 10000 psi.

900-24 Test 11 17 Apr 88

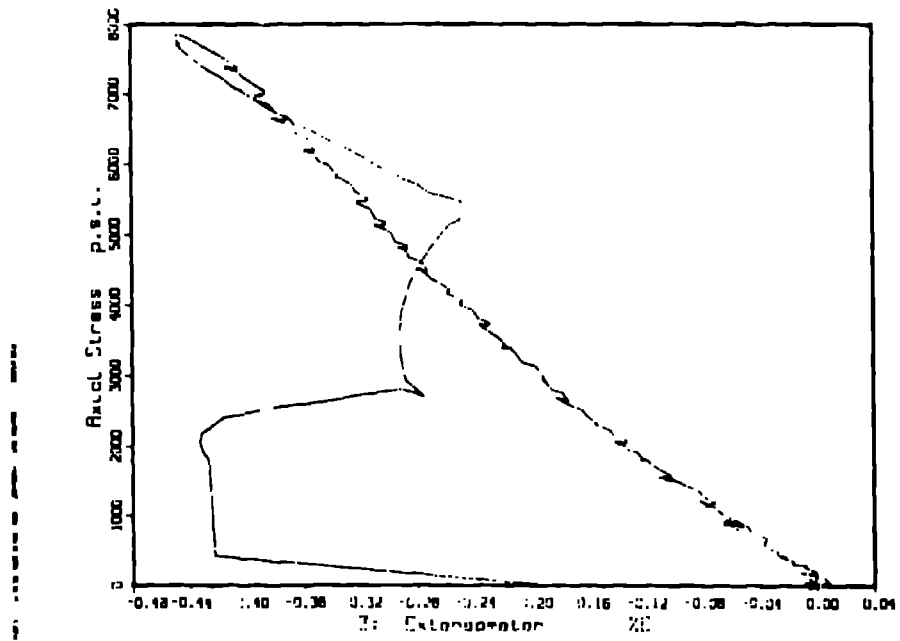


Figure 15: Dad test number 2.

900-24 Test 12 13 Apr 88

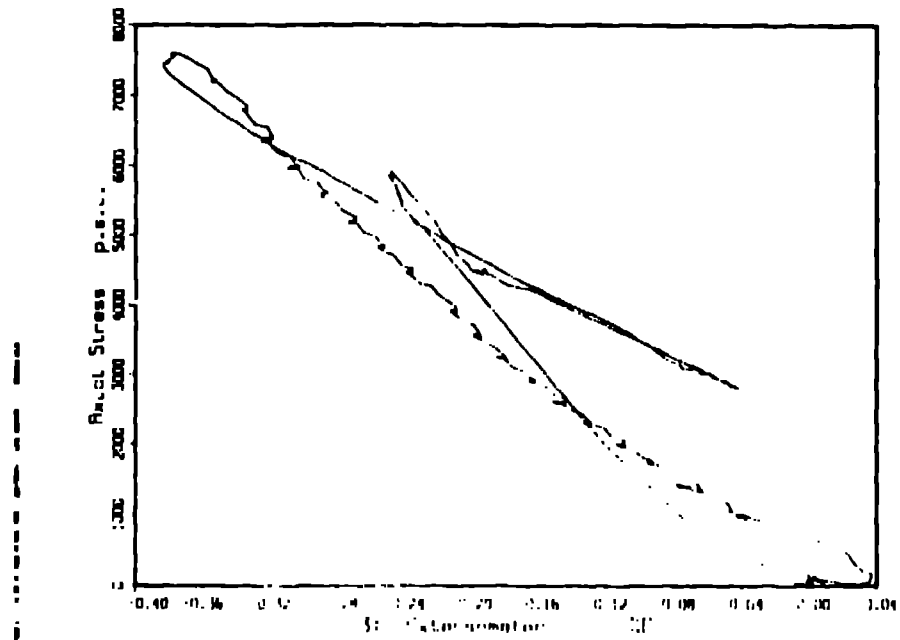


Figure 10: Tens-Lac undercoat and overcoat, 7251 psi. The overcoat is a clear flexible coating used to protect the undercoat.

900-24 Test 13 13 Apr 88

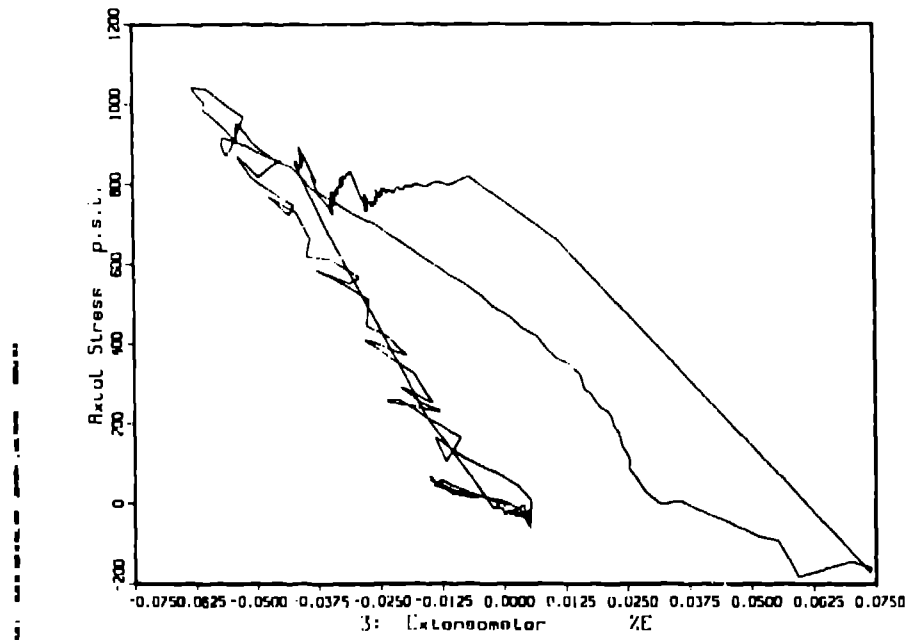


Figure 17: Uncoated specimen 4, 725 psi. This sample is close to the conditions in a standard tension test with only atmospheric confining pressure.